

Fabrication of flexible supercapacitors with high electrochemical performance

Haojie Fei, Ph.D.

Doctoral Thesis Summary



Tomas Bata University in Zlín

Faculty of Technology

Doctoral Thesis Summary

Fabrication of flexible supercapacitors with high electrochemical performance

Výroba flexibilního superkondenzátoru s vysokým elektrochemickým výkonem

Author: **Haojie Fei**

Study Programme: Chemistry and Materials Technology P 2808

Study Course: Technology of Macromolecular Compounds 2808V006

Supervisor: Prof. Petr Sába

Consultants: Assoc. Prof. Nabanita Saha and Ing. Robert Moučka, PhD

External examiners: Dr. Irina Sapurina, CSc.
Ing. Mária Omastová, DrSc.
prof. Ing. Otakar Bokůvka, Ph.D.

Zlín, February 2018

© Haojie FEI

Published by **Tomas Bata University in Zlín** in the Edition **Doctoral Thesis Summary**.

The publication was issued in the year 2018.

Key words: *flexible supercapacitor, reduced graphene oxide, pseudo-capacitive material, hydrogel electrolyte*

Klíčové slova: *flexibilní superkondenzátor, redukováný grafenoxid, hydrogel elektrolyt, pseudo-kapacitní materiály*

Full-text of the doctoral thesis is available in the Library of TBU in Zlín.

ISBN 978-80-7454-725-6

Résumé

Flexibilní superkapacitory představují slibné zařízení pro ukládání elektrické energie v přenosné elektronice. Vývoji flexibilního superkapacitoru s dobrými elektrochemickými vlastnostmi, jako je vysoká proudová hustota, výkon a životnost je v současné době věnována značná pozornost. K dosažení tohoto cíle je třeba nicméně překonat překážky jak při přípravě pružných elektrod a pevných elektrolytů tak při navrhování a výrobě flexibilních superkapacitorů. Tato práce je zaměřena na výrobu flexibilních superkapacitorů s vysokým elektrochemickým výkonem, které jsou založeny na hydrogelu na bázi redukovaného grafenoxidu (RGO). K tomuto účelu byly připraveny dva druhy kompozitních elektrod založených na hydrogelu na bázi RGO s redox aktivními látkami; první typ využívá polyanilín (PANI), druhý pak oxid mangančitý (MnO_2). Dále byly připraveny gelové/hydrogelové elektrolyty vhodné pro daný flexibilní superkapacitor. V práci jsou diskutovány klíčové faktory ovlivňující flexibilitu finálních zařízení. Samotné zlepšení flexibility připravených superkapacitorů bylo dosaženo dvěma způsoby, a to jednak konfigurací s volným pohybem a jednak snížením tloušťky celého zařízení.

Summary

Flexible supercapacitors (SCs) are one kind of promising energy storage device for portable electronics. To gain a supercapacitor with high flexibility and electrochemical performance, such as high energy density, power density and cycling stability has drawn massive attention. However, to achieve this goal, there are challenges in the preparation of flexible electrodes and solid-state electrolyte as well as the design and fabrication of flexible SCs. This doctoral thesis work is focused on the fabrication of flexible SCs with high electrochemical performance based on reduced graphene oxide (RGO) hydrogel. Two composite RGO hydrogel film electrodes with redox-active materials, polyaniline (PANI) or manganese dioxide (MnO_2) were prepared. Suitable gel/hydrogel electrolytes were prepared to match the designs for each flexible supercapacitor. In the study, important factors on the flexibility of final devices have been discussed. Two strategies, free-movement configuration and the reduction of the thickness of entire devices were applied to improve the flexibility of the assembled SCs.

Contents

RÉSUMÉ	3
SUMMARY	3
ABSTRACT	5
1. INTRODUCTION	6
2.1 Principles of Capacitor	6
2.2 Electrochemical double-layer capacitors.....	7
2.3 Redox-active materials to increase capacitance	7
2.4 Asymmetric (hybrid) systems to achieve high energy density.....	8
2.5 Electrochemical characterization	9
3. FLEXIBLE SUPERCAPACITORS	9
3.1 Mechanical theory of the film-on-substrate structure	9
3.2 Structural design and optimization of flexible SCs.....	10
3.3 RGO hydrogel based flexible electrode	11
3.4 Gel/hydrogel electrolyte	12
4. AIMS OF DOCTORAL THESIS	12
5. EXPERIMENTAL	12
5.1 Materials and samples preparation	12
5.2 Characterization.....	14
6. RESULTS AND DISCUSSION	15
6.1 Polyaniline/reduced graphene oxide hydrogel film with attached graphite current collector for flexible supercapacitors	15
6.2 A highly flexible asymmetric supercapacitor using two dimensional nanomaterials and a bacterial cellulose filled neutral gel electrolyte.....	19
6.3 In-situ preparation of bacterial cellulose reinforced hydrogel electrolyte for flexible supercapacitors	23
6.4 Summary and outlook	25
BIBLIOGRAPHY	26
LIST OF FIGURES	29
LIST OF SYMBOLS AND ABBREVIATIONS	31
LIST OF PUBLICATIONS	32
CURRICULUM VITAE	33

Abstract

This doctoral thesis has mainly been divided into two parts, **theoretical part (Chapter 2 and 3)** and **research part (Chapter 5 and 6)**. Firstly, the thesis theoretically describes the following points: (i) general properties of SCs and (ii) general information about flexible SCs. At the former point, the advantage of SCs compared to the conventional capacitors and batteries is explained through the traditional electrochemical double-layer capacitors (EDLCs) following the capacitor principles (**Chapter 2.1 and 2.2**). Two popular ways to increase the energy density of SCs: the use of *pseudo-capacitive materials* (**Chapter 2.3**) and the development of *asymmetric configuration* (**Chapter 2.4**) are both described. The importance of structural design of active electrode materials and conductive additives on electrochemical performance are highlighted. Further, the measurements used to evaluate the electrochemical performance of electrodes such as cyclic voltammetry (CV), galvanostatic charge/discharge (GCD) and electrochemical impedance spectroscopy (EIS) are illustrated (**Chapter 2.5**). At the later point of flexible SCs, general information of the fabrication of flexible SCs has been introduced (**Chapter 3**). The mechanical theory of the film-on-substrate structure, regarded as the base of the fabrication of flexible electronics, is analysed, where three most important factors: (1) thickness, (2) flexible substrate and (3) mechanical neutral plane are emphasized (**Chapter 3.1**). Further, two widely used construction structures: (a) sandwich-type structure and (b) planar configuration are briefly introduced and compared (**Chapter 3.2**). The roles of RGO based flexible electrodes and gel/hydrogel electrolytes in flexible SCs are summarized. The advantages and disadvantages of RGO hydrogel electrode are also discussed (**Chapter 3.3 and 3.4**).

The research part has been divided into two sections, **Experimental, (Chapter 5)** and **Results and discussion (Chapter 6)**. Firstly, stable colloidal suspensions of RGO and MnO₂ were prepared. Based on these two colloids, two RGO hydrogel composite films with redox-active materials, PANI and MnO₂, were prepared, respectively. To improve the flexibility of the assembled SCs, two strategies, a free-movement configuration and the reduction of the thickness of entire devices were applied. Moreover, suitable gel electrolytes were prepared for the two constructional strategies. Finally, two flexible SCs were fabricated and characterized subsequently. In addition, for the study of hydrogel electrolyte, a mechanically strong hydrogel electrolyte was prepared and characterized.

Therefore, the study has been carried out with three directions and the results have been presented in three different sections, shown as **1) Chapter 6.1** “*Polyaniline/reduced graphene oxide hydrogel film with attached graphite current collector for flexible SCs*”, **2) Chapter 6.2** “*A highly flexible asymmetric SC using two dimensional nanomaterials and a bacterial cellulose*

filled neutral gel electrolyte”, and 3) **Chapter 6.2** “*In-situ preparation of bacterial cellulose reinforced hydrogel electrolyte for flexible SCs*”

1. INTRODUCTION

Recently, flexible electronics have drawn profound interest.¹ However, they are lack of flexible energy storage devices as their supplying power source.² Electrochemical capacitors (ECs) , also known as SCs, are one of the most promising candidates for energy storage devices because of their extremely long cycle life, fast charge/discharge, high power density and simple structures.³ However, conventional ECs are too heavy, thick and bulky to match flexibility.

Therefore, to gain electrodes with robust mechanical flexibility, high energy density, power density and excellent cycling stability is the key to the flexible energy devices. RGO is an ideal material for flexible electrodes due to its two-dimensional structure, high specific surface area(SSA) and electric conductivity, as well as their low-cost, partial functionalization, compared to graphene.⁴ However, the aggregation and restacking of individual graphene nanosheets in these films reduce their SSA and re-wettability to electrolyte, resulting in blocking the diffusion of ions and decreasing the electrochemical performance.⁵ RGO hydrogel films with a wet state have recently drawn massive attention.⁶

On the other hand, the combination of flexible electrodes with electrolytes and separators in the integral design and assembly of devices are important as well. A conventional flexible SC often consists of two flexible electrodes with current collectors separated by aqueous gel electrolyte. Since this classic sandwich-type flexible SC is constructed by piling up these components layer-by-layer, the large thickness of final SC device extremely hinders the flexibility. Therefore, optimizing the structural design of flexible SCs is required.⁷

This doctoral work is focused on the fabrication of flexible SCs with high electrochemical performance. To this end, flexible electrodes based on RGO hydrogel films modified by pseudo-active materials such as PANI and MnO₂ have been prepared. Suitable gel electrolytes were prepared at the point of view to match the construction and electrochemical performance of flexible SCs. Finally, the construction of flexible SC was designed and investigated accordingly. The design of flexible SC is studied during the fabrication.

2. GENERAL PROPERTIES OF ELECTROCHEMICAL CAPACITORS

2.1 Principles of Capacitor

A capacitor is a passive component that stores energy in an electrostatic field. It is composed of two parallel electrodes (plates) separated by a dielectric. When applying a potential difference between these two electrodes, positive and negative charges migrate toward the surface of opposite polarized electrodes to

be in a charged state. Once this charged capacitor is connected in a circuit, it can act as a voltage source for a short period.⁸ As the following Equation (1), its capacitance (C) is the ratio of the electric charges stored in each electrode (Q) to the potential difference between them (V).

$$C = Q/V \quad (1)$$

For a typical parallel plate capacitor, C is proportional to the area (A) of each electrode and the permittivity (ε) of the dielectric and inversely proportional to the distance (d) between the two electrodes, expressed as:

$$C = \varepsilon_0 \varepsilon_r A/d \quad (2)$$

where ε_0 stands for the permittivity of free space and ε_r represents the dielectric constant (or relative permittivity) of the material between two plates. Two primary attributes of a capacitor are its energy and power density (specific energy or power), both of which can be expressed as a quantity per unit weight or per unit volume or unit area. The energy E (J) is directly proportional to its capacitance and the square of the potential difference (V):

$$E = 1/2 CV^2 \quad (3)$$

$$P = E/t \quad (4)$$

In general, average power (P) is the rate of energy delivery per unit time (t) as above Eq. (4). The power for a capacitor is usually measured at the matched impedance⁹ which corresponds to the maximum power $P_{max.}$, expressed as

$$P_{max.} = V^2/4ESR \quad (5)$$

The internal resistance of a capacitor (ESR) includes the resistances of the components within a capacitor such as the electrode materials, current collectors, dielectric or electrolyte and separators.

2.2 Electrochemical double-layer capacitors

EDLCs store charge electrostatically by reversible ion adsorption occurring at the electrode/electrolyte interface. In the charged state, charges are separated and form a structure called “double layer” at the interface.¹⁰ The electrodes of EDLCs have much higher effective surface area (A) and thinner dielectric in “double layer” (d), it results in a significant increase of both capacitance and energy than those of regular capacitors (Equation (2)). The key to achieve high capacitance by electrostatic charge storage is to use those electrode materials with high SSA and electric conductivity. However, in reality, the relationship between specific capacitance and SSA does not follow a linear trend. The capacitance increase was limited even for most of highly porous samples.

2.3 Redox-active materials to increase capacitance

Therefore, metal oxides and conducting polymers have been used in ECs, since these materials utilize fast and reversible redox reactions at their surface.¹¹

It represents a different kind of capacitance contribution to double-layer capacitance. This kind of ECs is usually called pseudo-capacitors, which possess higher energy density than EDLCs. But because redox reactions are used, like batteries, they often suffer from weakness of short cycling stability. Since the reactions occur only on or close to the interface of electrode and electrolyte, the low surface area of conventional pseudo-capacitive materials and slow ion diffusion in their bulk electrode highly reduce the interface for these reactions. In addition, the low electric conductivity of most pseudo-capacitive material hinders the transfer of electrons within the electrodes as well. Thus, to achieve high-energy and high-power pseudo-capacitors, it is necessary to facilitate both the ionic and electronic currents within the electrodes by optimizing the design of nanostructured pseudo-capacitive materials on high SSA and electric conductive scaffold as shown in Figure 1.¹²

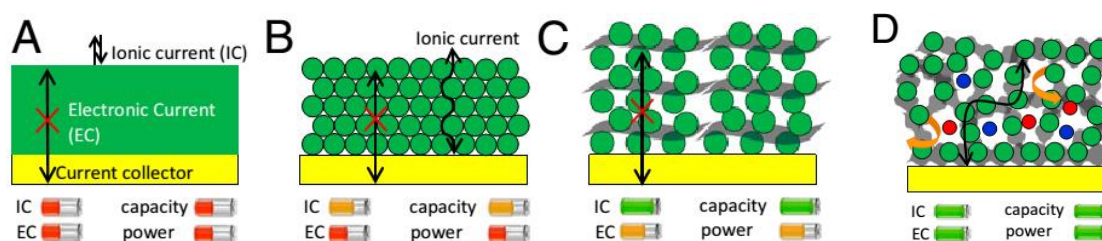


Figure 1 Rational design of supercapacitor electrodes with high energy and high power. Improving the ionic current (IC) and electronic current (EC) within the electrode is a key. Different approaches have been explored including (A) compact thick films of pseudo capacitive materials; (B) nanostructured pseudo capacitive material films; (C) addition of conductive materials to the nanostructured pseudo capacitive materials; and (D) recent approach of growing nanostructured pseudo capacitive material on 3D interconnected networks with high surface area and high electronic conductivity.¹²

2.4 Asymmetric (hybrid) systems to achieve high energy density

The maximum energy density ($E_{max.}$) is expressed as

$$E_{max.} = 1/2 C U_{max.}^2 \quad (6)$$

and is proportional to the square of the maximum operating voltage ($U_{max.}$) of the cell, which is determined on the materials used for the electrode and electrolyte. Aqueous electrolytes possess a great amount of advantages such as their small ionic radius and high ionic conductivity. In addition, aqueous electrolyte based ECs can be fabricated in moderate atmosphere conditions. The rapid development of electrode materials now enables a new class of ECs in which two distinct electrodes are paired in an asymmetric configuration. A “pseudocapacitive” (MnO_2) material is the positive electrode and a high surface-area carbon is the negative electrode. In such configuration, the high overpotentials for H_2 and O_2 evolution at the carbon-based negative electrode and pseudocapacitive positive electrode, respectively, extend the limit of

potential window of aqueous electrolytes, resulting in significantly higher specific energy than for symmetric aqueous-based ECs.¹³

2.5 Electrochemical characterization

The electrochemical performance of ECs is measured by an electrochemical workstation. There are two test fixture configurations for the electrochemical cell, two-electrode and three-electrode configurations. For a two-electrode cell, the voltage measured (or controlled) is the cell voltage since the counter electrode (CE) and the reference electrode (RE) are shorted. For a three-electrode cell, a RE electrode is added, which exhibits a constant potential over a large range of currents. In this way, the voltage of working electrode (WE) is able to be accurately measured (or controlled).¹⁴ Three most used electrochemical methods are cyclic voltammetry (CV), galvanostatic charge/discharge (GCD) and electrochemical impedance spectroscopy (EIS).

3. FLEXIBLE SUPERCAPACITORS

3.1 Mechanical theory of the film-on-substrate structure

Most flexible SCs mean that they are bendable. To fabricate high bendable electrodes which can properly work under a large degree of bending is the key for flexible SC devices. To this end, the mechanical analysis of electrode materials on flexible substrates is crucial and regarded as the theoretical basis for the design and implementation of flexible SCs.

Figure 2 illustrates a bent film deposited on a compliant substrate (a multilayer film structure). It is the same structure as the conventional electrodes where the active material deposited on flexible substrates or metal current collectors.³ As can be seen, the inner surface is compressed, while the outer surface is tensed. Strain in the film is mainly caused by an external bending moment. When the deposited film and the compliant substrate have the same Young's modulus, the strain in the top surface (ε_{top}) is as follows:¹⁵

$$\varepsilon_{top} = (d_f + d_s)/2R \quad (7)$$

where the thickness and Young's moduli of the deposited film and the substrate are d_f and d_s , Y_f and Y_s , respectively. R is the bending radius. When the film and the substrate have different moduli ($Y_f > Y_s$), the neutral plane moves toward the more rigid film. (The neutral plane is a surface within film, where the material is not under stress, either compressive or tensile.) and the ε_{top} is given by

$$\varepsilon_{top} = \left(\frac{d_f + d_s}{2R} \right) \frac{(1 + 2\eta + \chi\eta^2)}{(1 + \eta)(1 + \chi\eta)} \quad (8)$$

where $\eta = d_f/d_s$ and $\chi = Y_f/Y_s$.

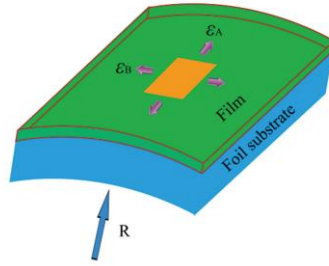


Figure 2 A multilayer film structure bending into a cylindrical roll.³

Importance of Thickness

According to Equation (9), the critical bending radius (R) scales linearly with the total thickness ($d_f + d_s$). Recently, lots of nanomaterials such as CNTs, graphene, nanowires and other nanosheets have attracted wide interest, owing to their high mechanical flexibility that originates from interconnected structures when they are stacked layer-by-layer to form a thin film.

Use of flexible substrates

When the Young's moduli of the flexible substrate is much smaller than that of the active materials deposited film, the mechanical neutral plane moves toward to the deposited film, resulting in decreasing the stress.^{16, 17} Thus, recently, more flexible substrates such as various polymers, cellulose papers, CNT films and graphene films have been widely used to support active materials and buffer built-in stress during bending.

Effect of mechanical neutral plane

Another deduction from the above Equations (7) and (8) is that the strain in a film can be further reduced if the film is sandwiched between an encapsulation and a substrate layer with a suitable Young's modulus Y_e and thickness d_e .³ When $Y_s d_s^2 = Y_e d_e^2$, the rigid film itself acts as the neutral plane.^{3, 16} In this case, bending does not add any strain to the film, and the whole structure can be bent to an extremely small radius.

3.2 Structural design and optimization of flexible SCs

The most common structure for flexible SC is sandwich-type SC, as shown in Figure 3 (left). This type SC is constructed by layer-by-layer piling the electrodes, electrolyte (separator) and current collectors, which is a simple fabrication method. It is the popular fabrication method for free-standing electrode films with a large scale up to several centimeters. The deposition of the active electrode materials is usually larger than the planar configuration, resulting in a higher areal capacitance. To this end, it requires the free-standing electrode to obtain much strong mechanical properties.

On the other hand, as we know, the conductivity of the electrode is generally too low to serve itself as the current collector. Thus, flexible current collectors

have to be paid more attention in the sandwich-type fabrication of flexible SCs. Based on this point, the interactions between the electrode film and the flexible current collector and their behaviors during the bending also are worthy to study. Another challenge of flexible current collectors is the corrosion of metals in aqueous electrolytes. The use of noble metals reduces the advantage of low-cost of aqueous electrolyte based supercapacitors.

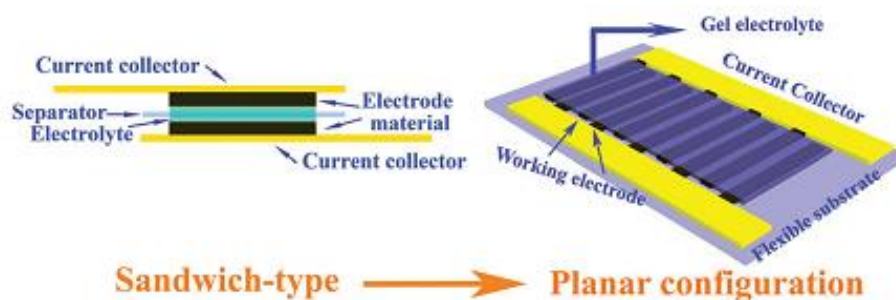


Figure 3 Schematic comparison of the sandwich-type supercapacitor (left) and planar supercapacitor (right).⁷

The most disadvantage of this structure is that the entire device is thick, which reduces its flexibility as be discussed in section 3.1 above. Even worse, the deformation behavior of this sandwich structure during the bending is more complicated due to the soft layer of gel/hydrogel electrolyte in the middle.¹⁸

3.3 RGO hydrogel based flexible electrode

RGO have been extensively studied as electrode materials for flexible electrodes due to their two-dimensional nanosheet structure, high SSA, and excellent flexibility, as well as their easy access, partial functionalization and low-cost, compared to graphene.¹⁹ By various methods, RGO self-supporting films could be prepared with robust mechanical strength.²⁰ However, during the drying process, aggregation and restacking of individual graphene nanosheets reduce the specific surface area of these obtained films and their re-wettability to electrolyte, decreasing the electrochemical performance.⁵ Thus, RGO hydrogel films have recently drawn M attention since their highly porous structure stores abundant electrolyte and provides continuous pathway for electrolyte ions.^{21, 22}

However, due to the limited capacitance contribution of electric double layer, the capacitance values of RGO hydrogel films are still lower compared to these of pseudocapacitors. In this case, pseudocapacitive materials are common to be employed into.^{23, 24} On the other hand, the defects on graphene nanosheets caused by oxidation degrade their qualities, especially their electrical conductivity. In consequence, electronic transport in these films cannot meet the demand for devices, especially for these who have large-scale electrodes and intend to work at high current. Therefore, current collectors are still extremely necessary. Moreover, since the restacking of RGO nanosheets is reduced in RGO hydrogel, their mechanical property is lower than RGO free-standing

films. Thus, the fabrication method or the structural design and optimization of flexible SCs are necessary to take into consideration.

3.4 Gel/hydrogel electrolyte

Due to the deformation of flexible SCs, the leakage of liquid electrolyte aggravates. Rather than improving the sealing technique, the use of solid state electrolyte is more practical. In case of aqueous electrolyte, the gel or hydrogel electrolyte are generally used.²⁵⁻²⁷ Generally, the gel electrolyte is prepared by dissolving suitable polymers into aqueous electrolyte to form gels with high viscosity. However, these gels usually are just cross-linked by physical hydrogen bond, which can be broken down when the temperature increases. Hydrogel electrolyte is a hopeful candidate since it can hold enormous aqueous electrolyte, which makes sure that it has a similarly high ionic conductivity corresponding to the aqueous electrolyte, but remains in a quasi-solid state even at high temperature due to their chemical crosslinking.²⁸ Recently, material scientists are developing various polymer hydrogels as solid electrolytes for flexible SCs.^{29, 30} Unfortunately, most of them are lack of mechanical property as they contain too much water. In addition, the hydrogel electrolyte is a form of membrane, which has a bad interaction between the electrodes and them. The adhesion of electrode and electrolyte can be easily destroyed, especially in the bend state of the flexible SCs. One of the strategies to solve this problem is to in situ polymerize the hydrogel electrolyte directly between two electrodes in presence of electrolyte solution and reinforcing materials. Two electrodes would be united as a whole and flexible SCs could be assembled.

4. AIMS OF DOCTORAL THESIS

To achieve the goal of the fabrication of flexible SCs with high electrochemical properties, the work has been divided into several parts.

1. Preparation of flexible electrode materials: (i) preparation of highly conductive and porous RGO hydrogel film, (ii) modification of RGO hydrogel film by pseudo capacitive materials such as PANI and MnO₂.

2. Preparation of gel/hydrogel electrolytes for the fabrication of flexible devices.

3. Design of flexible device according to the properties of obtained composite electrodes and gel/hydrogel electrolytes.

4. Fabrication of flexible device and investigation of its electrochemical performance and flexibility.

5. EXPERIMENTAL

5.1 Materials and samples preparation

Preparation of GO, RGO and MnO₂ colloidal suspensions

Graphite oxide was prepared by the oxidation of natural graphite flakes (325 mesh, Graphite Tyn) according to a modified Hummers' method.³¹ MnO_2 colloidal suspension was prepared according to a previous literature.³²

Preparation of RGO/G, PANI/RGO/G and MnO_2 /RGO/G hydrogel films

RGO hydrogel films were prepared by vacuum filtration of RGO colloid. To obtain a graphite current collector on RGO/G, at the end of the filtration, graphite suspension was added into until the filtration completed.

PANI/RGO/G hydrogel films were obtained by in-situ polymerization of aniline onto an RGO/G. Finally, the films were compressed between two pieces of polyvinylidene fluoride (PVDF) filter membranes under 10 MPa.

MnO_2 /RGO hydrogels were prepared by vacuum filtration of mixed MnO_2 /RGO colloid. A graphite current collector was deposited on these hydrogels by successive filtration of graphite flakes suspension. The desired flexible hydrogel electrodes were obtained by compressing these hydrogels between two pieces of PVDF filter membranes under 15 MPa.

Preparation of the BC modified PAAS- Na_2SO_4 gel electrolyte

Polyacrylic acid sodium salt (PAAS) gel was synthesized by the radical polymerization of acrylic acid in water. Typical procedure was as follows: 3.5 g acrylic acid was neutralized by NaOH in 8 mL deionized water. Then 1.95 g potassium persulfate ($\text{K}_2\text{S}_2\text{O}_8$) was added in this solution. The polymerization was conducted at 85 °C with stirring and in N_2 atmosphere to gain PAAS gel. Then, 20 g wet BC membrane was grinded into BC clusters and precipitated by a centrifuge with the speed of 8000 rpm (Rotina 380, Hettich). The BC precipitation and 3.98 g Na_2SO_4 were mixed with previous PAAS gel electrolyte to obtain BC/PAAS- Na_2SO_4 gel electrolyte.

Fabrication of flexible SC using PANI/RGO/G hydrogel films

The packing substrate (poly(dimethyl siloxane), (PDMS) of the device was prepared from SYLGARD ® 184 (Dow Corning Corporation). It represents a slide (thickness = 0.2 cm) with a cavity (2.5 cm long, 1.3 cm wide, 0.15 cm deep). Two prepared PANI/RGO/G films were put into the cavity, separated and surrounded by poly(vinyl alcohol)- H_2SO_4 (PVA- H_2SO_4) gel electrolyte (10 g PVA (M_w , ~ 145,000) dissolved in 90 g 1 M H_2SO_4 solution). Two titanium foils were placed on each edge of the films with an area of 1 cm × 0.5 cm. This part of the films was pre-dried on a hot plate for seconds at a temperature of about 80 °C and separated by Parafilm. The effective electrode area was 1 cm × 1.5 cm. Then a polyethylene terephthalate (PET) substrate was put on the top for sealing. Finally, the titanium foils were fixed by a clip.

Fabrication of the flexible SC using RGO/G and MnO_2 /RGO/G hydrogel film

Compressed RGO/G and MnO₂/RGO/g hydrogel films were cut to a size of 3 cm × 1 cm with a tail of 1.25 cm × 0.3 cm for the connection with titanium foils. Each piece of RGO and MnO₂/RGO hydrogel films was placed on the polyethylene (PE) films (40 μm, thickness). Then, they were assembled face to face, separated by BC modified PAAS-Na₂SO₄ gel electrolyte with a traditional sandwich-type structure. Finally, they were compressed under 0.5 MPa between two flat plates to obtain the flexible SC device.

Preparation of hydrogel electrolytes

Procedure for the preparation of hydrogel electrolytes was as follows: 3.6 g acrylic acid was dissolved in 2.5 mL water and neutralized by 2.86 g KOH. Then, 1 g poly(ethylene glycol) diacrylate (PEGDA), 0.06 g CaSO₄·H₂O, 7.5 g BC suspension (0.2 wt. %) and 25.6 mg (Potassium persulfate) KPS was added into this solution. Finally, the obtained solution was dropped into 18.4 g sodium alginate (SA) solution (5 wt. %) under stirring. The mixture was casted into a mold and kept in the oven for 1 h at 80 °C. The gained hydrogel was immersed into 1 M CaCl₂ solution for 2 days and then in 2 M KCl for 1 day. SA crosslinked by CaSO₄·H₂O was designated as “SA-CaSO₄”, and crosslinked by CaSO₄·H₂O and CaCl₂ was named as “SA-Ca”.

5.2 Characterization

The morphology and structure of obtained nanomaterials and their composite films were characterized by Atomic force microscopy (AFM, Dimension Icon, Bruker), scanning electron microscopy (SEM, FEI Nova NanoSEM450), transmission electron microscopy (TEM, JEOL JEM-2100) and X-ray diffraction (XRD, Rigaku MiniFlex 600). The Raman spectra were obtained using a Raman spectrometer (Jobin-Yvon, LabRam HR). The Zeta potentials of MnO₂ and RGO in colloidal suspensions were measured by Zetasizer Nano ZS90 (Malvern). The rheology behavior of PAAS-Na₂SO₄ gel electrolyte was examined by the Rheometer MCR 502 (Anton-Paar). The resultant hydrogel was characterized by ATR-FTIR (Nicolet iS5). The compression test was conducted by Testometric MT350-5CT.

The electrochemical characterization was carried out by cyclic voltammetry (CV), galvanostatic charge-discharge test and electrochemical impedance spectroscopy (EIS) using Autolab PGSTAT128N (Metrohm, Netherlands). The electrochemical performance of the prepared hydrogel films was first investigated in a three-electrode system with an Ag/AgCl reference electrode and a Platinum counter electrode. The specific capacitance of the electrodes from CV profile (C_{sp}) was calculated using the following equation:

$$C_{sp} = \int I dU / 2vm\Delta U \quad (9)$$

where I is the current, $\int I dU$ is the integration area for the CV curve, v is the scan rate, m is the mass of the active material, ΔU is the potential window, the

factor 2 corrects the fact that above integration area includes both the positive and negative scan. The measurement for assembled devices was carried out in a two-electrode system. The specific capacitance of each device was calculated from the galvanostatic curves at different current densities using the formula:

$$C_t = I\Delta t/m\Delta V \quad (10)$$

where I is the discharge current, Δt stands for the discharge time, m is the total mass of active materials in both electrodes (without graphite current collectors), and ΔV is the voltage drop upon discharging (excluding IR_{drop} , the potential drop at the beginning of the discharge in charge-discharge profile). The areal capacitance (C_A) of each device was calculated by following equation:

$$C_A = C_t/A, \quad (11)$$

where A is the footprint area of the electrodes. For the symmetric cells, the specific capacitance (C_{sc}) of one electrode was calculated following the equation:

$$C_{sc} = 4C_t \quad (12)$$

Finally, the energy density (E) and power density (P) of each device was derived from the equation:

$$E = C_t\Delta V^2/2 \quad (13)$$

$$P = E/\Delta t \quad (14)$$

6. RESULTS AND DISCUSSION

6.1 Polyaniline/reduced graphene oxide hydrogel film with attached graphite current collector for flexible supercapacitors

Here, a flexible SC based on PANI/RGO/G hydrogel films was prepared. A graphite current collector was directly deposited on the surface of RGO hydrogel films and modified by PANI through a diluted in-situ polymerization. During the fabrication of the SC, a new structural design of the SC was adopted to solve the problem of weak mechanical properties of RGO hydrogel films. As a result, high electrochemical performance has been achieved due to (i) the high diffusion of electrolyte ions in hydrogel films, (ii) the contribution of high pseudocapacitance of PANI, and (iii) the enhanced electron transport endowed by graphite current collectors. Moreover, owing to the special design, this SC exhibits high flexibility. This study shows a promising possibility for the application of RGO hydrogel based films in flexible SCs.

A graphite flakes were deposited on one side of RGO hydrogels, serving as a current collector after successive filtration of RGO dispersion and graphite suspension. After compressing, graphite flakes are strongly attached to RGO matrix; it also improves their flexibility and mechanical properties. RGO film exhibits porous structure, providing continuous ionic pathways across piled

RGO layers (Figure 4a). Importantly, RGO flakes stand on the surface, from the side perspective (Figure 4b). That is why graphite flakes can be embedded into the RGO film during the filtration and then held tightly after compression. Figure 4h shows a layer-by-layer structure with a highly porous structure. Figure 4f and 4i confirms that PANI nanoarrays are present not only on the surface but also inside the hydrogel. Such fine growth of PANI nanoarrays and their uniform distribution benefit from the interconnected channels within hydrogel as well as from the low concentration of aniline in the reaction media.³³

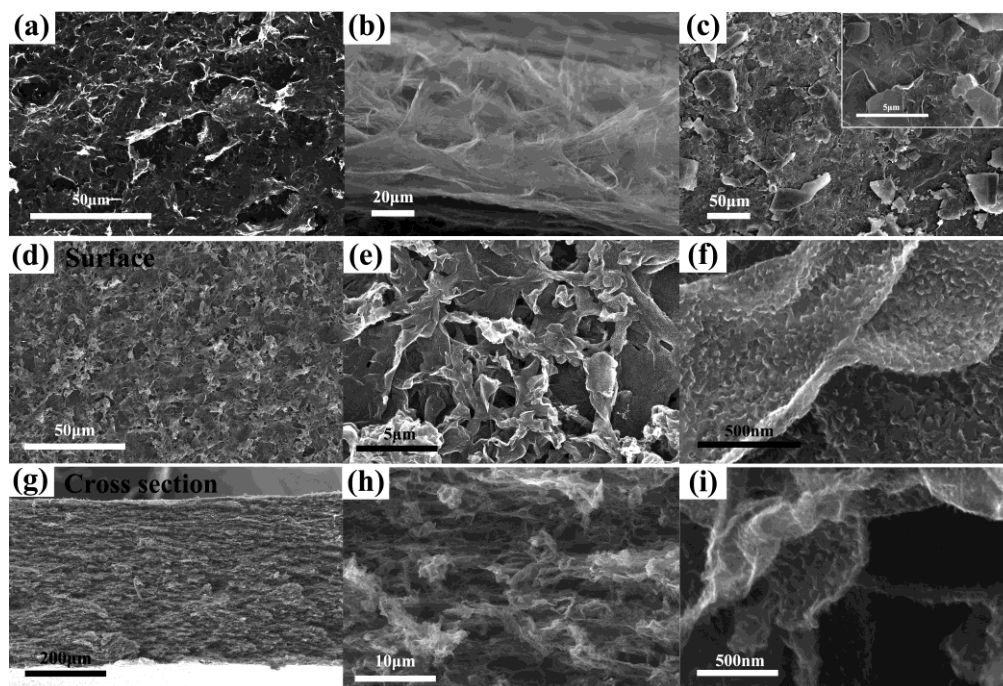


Figure 4 SEM images of the surface of RGO hydrogel from (a) top view and (b) side perspective, (c) the surface of graphite side of RGO/G film (inset image shows its high magnification image), (d) the surface of PANI/RGO hydrogel and (e, f) at high magnification, (g) the cross-section of PANI/RGO hydrogel and (h, i) at high magnification.

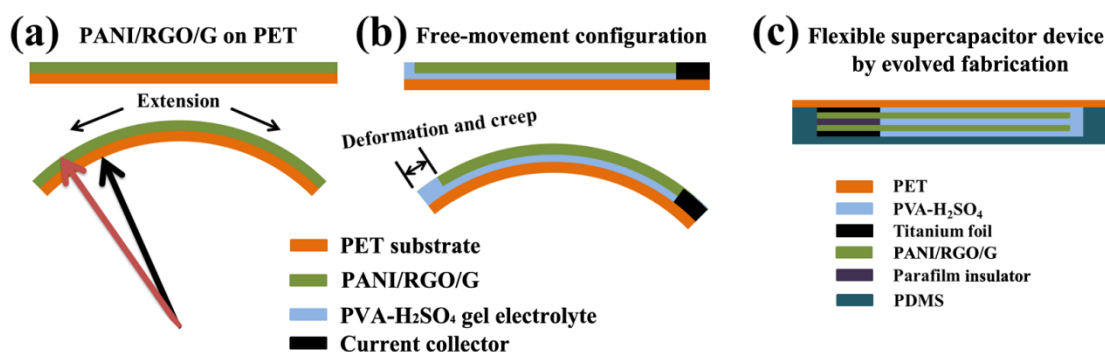


Figure 5 (a) Schematic diagram of PANI/RGO/G hydrogel film on a PET substrate and the different extensions upon the radius caused by bending. (b) Free-movement configuration and its mechanism to reduce the stress force during bending. (c) Illustration for constructing flexible supercapacitor devices using a free-movement configuration (cross section).

However, during the fabrication of flexible SCs, hydrogel films exhibit weak mechanical properties. Structural design plays an important role on the flexibility of devices. Therefore, an alternative SC fabrication approach was adopted. The schematic diagram is shown in Figure 5. As can be seen, when the multilayer of PANI/RGO/G and PET substrate gets bent, the lengths are getting different upon the radius from the center of concentric circles (Figure 5a). The top of PANI/RGO/G is stretched.¹⁶ Since PANI/RGO/G has a low tensibility, it tends to be torn up. Therefore, a free-movement configuration was adopted (Figure 5b). PANI/RGO/G and the PET substrate are separated by PVA-H₂SO₄ gel electrolyte, and only one side of PANI/RGO/G is provided with current collector. As a result, due to the deformation and creep of gel electrolyte, PANI/RGO/G can freely move when bent, the stress applied to PANI/RGO/G from gel electrolyte is much lower than that from PET substrate. This configuration has been adopted to assemble the flexible SC (Figure 5c).

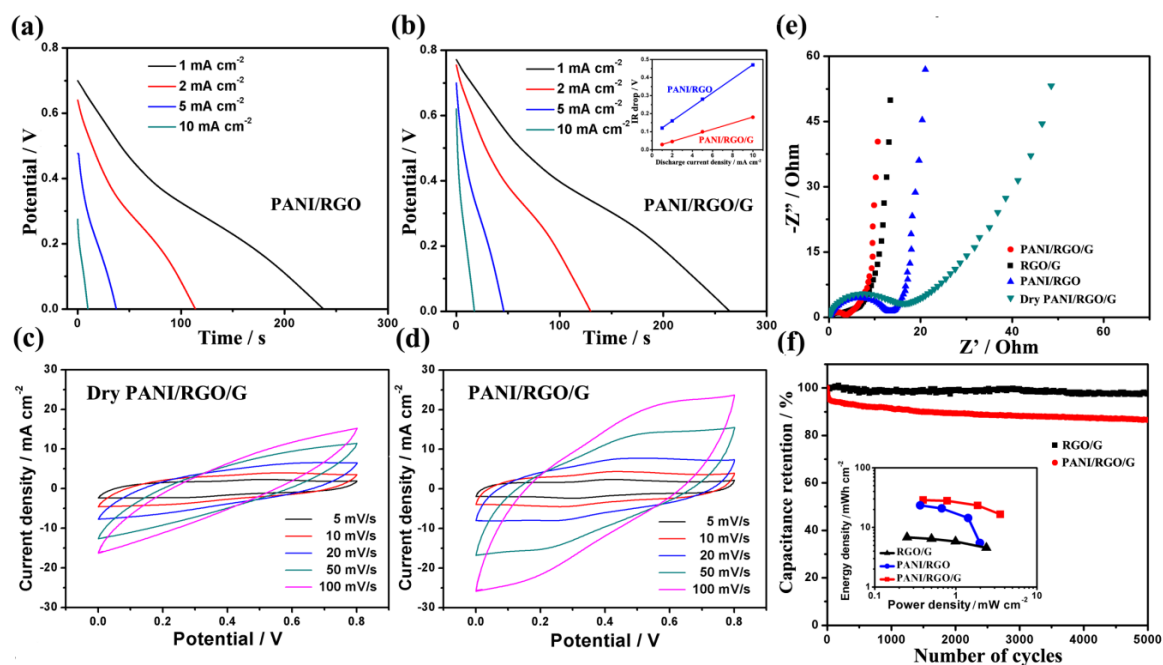


Figure 6 Electrochemical performance of symmetric flexible devices using various prepared films. Galvanostatic discharge curves of (a) PANI/RGO and (b) PANI/RGO/G devices at various current densities from 1 mA cm⁻² to 10 mA cm⁻²; inset graph shows the summary of their IR_{drop} vs current densities. Cyclic voltammograms of (c) dry PANI/RGO/G and (d) PANI/RGO/G hydrogel film device at different scan rates from 5 mV s⁻¹ to 100 mV s⁻¹. (e) Nyquist plots demonstrate the effect of graphite current collector and wet-state of the films on R_{cr} . (f) Cycling stability of RGO/G and PANI/RGO/G devices at a high current density of 5 mA cm⁻² (inset image shows their areal energy densities vs average power densities).

Electrochemical performance of assembled flexible SCs with various hydrogel films was subsequently characterized. Firstly, the effect of a graphite current collector was studied. Figures 6a and 6b show the galvanostatic discharge profiles of PANI/RGO and PANI/RGO/G at various current densities.

Each IR_{drop} of PANI/RGO/G is extremely lower than that of PANI/RGO for the corresponding current density. Because of PANI, PANI/RGO/G exhibits a much higher specific gravimetric capacitance (C_{sc}) of 409 F g^{-1} (478 F g^{-1} , excluding the mass of graphite current collector) at 2 mA cm^{-2} , compared to that of RGO/G (110 F g^{-1} and 152 F g^{-1} , respectively). The PANI/RGO/G device yields a gravimetric capacitance (C_t) of 120 F g^{-1} based on the total mass of two electrodes, and an areal specific capacitance of 352 mF cm^{-2} at 2 mA cm^{-2} , which is much higher than that of RGO/G (49 mF cm^{-2}).

The CV profile of dry PANI/RGO/G (Figures 6c) is distorted and turns to be spindle-like as the scan rate increases (from 5 to 100 mV s^{-1}), while that of PANI/RGO/G hydrogel film (Figures 6d) exhibits much better retention. This is attributed to the high ion transport in the RGO hydrogel. This is confirmed in Figure 6e, which shows the impedance curves of assembled SCs with various films. The charge transfer resistance (R_{ct}) of PANI/RGO/G, extracted from the intercept of the low-frequency impedance spectrum with the real axis, is 3.5Ω , which is almost the same as that of RGO/G but much lower than those of PANI/RGO and dry PANI/RGO/G. This indicates that the graphite current collector reduces the resistance of the films and that the interconnected porous structure of hydrogel films ensures fast ion diffusion.¹²

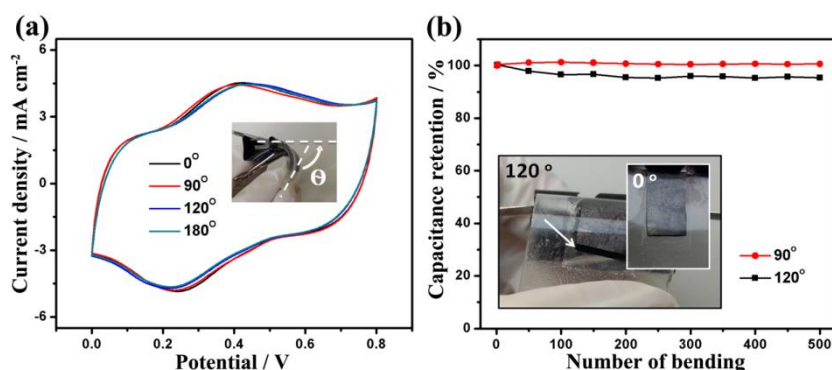


Figure 7 Flexibility of PANI/RGO/G device using a free-movement configuration. (a) Cyclic voltammograms at various bending angles at 10 mV s^{-1} . (b) Capacitance retention after various bending cycles at angles of 90° and 120° (inset image shows the deformation of gel electrolyte).

The flexibility of the fabricated SCs and its influence on the electrochemical performance were investigated further. Figure 7a shows that only a slight change can be observed on the CV curves, when the bending angle is from 90° to 180° . The capacitance retentions of the device after different numbers of bending are presented in Figure 7b. When the bending angle keeps at 90° , the device has almost the same capacitance as the initial one even after 500 times of bending. The obtained results confirm the improved flexibility achieved by using a free-movement configuration. The inset digital image in Figure 7b shows that when the bending angle turns from 0° to 120° , the gel electrolyte is sheared by two

parallel films on each side. The films keep their initial length, the elongation occurring in the gel electrolyte. Due to the high deformation and creep of the gel electrolyte, a slight shear force is applied to the hydrogel films.

6.2 A highly flexible asymmetric supercapacitor using two dimensional nanomaterials and a bacterial cellulose filled neutral gel electrolyte

In this study, a flexible asymmetric SC has been assembled using MnO_2/RGO (positive electrode) and RGO hydrogel films (negative electrode). A novel bacterial cellulose (BC) clusters filled polyacrylic acid sodium salt- Na_2SO_4 (BC/PAAS- Na_2SO_4) gel electrolyte was used to reduce the thickness of electrolyte layer, where BC cutlers filled in the gel can prevent from the contact of two electrodes during the compression. The assembled flexible cell exhibits high flexibility in sandwich-type construction, benefiting from the thin gel electrolyte layer as well as the use of 2D nanomaterials pillled flexible electrodes. It also displays good electrochemical performance due to the asymmetric configuration and high ionic diffusion in hydrogel electrodes. This device is very environmentally friendly, safe and low cost due to the appropriate selection of electrode materials and electrolyte.

In order to prepare RGO and MnO_2/RGO hydrogel films through the vacuum filtration, stable RGO and MnO_2/RGO colloidal suspensions have to be obtained. Figure 8a shows the photograph of RGO and MnO_2 colloidal suspensions and their mixture, respectively. They demonstrate the Tyndall effect, which indicates their colloidal behavior. The lamellar structures of RGO and MnO_2 were evident from their AFM and TEM images (Figure 8). The height profile scans of AFM images of MnO_2 and RGO (Figure 8b and c) present a fairly flat surface of both samples with approximate thicknesses of 4.5 nm and 1.3 nm, respectively. The lateral size of RGO is much larger than MnO_2 (Figure 8d and 8e). RGO sheets with large area and flat morphology serve as ideal microscopic substrates to host the MnO_2 . Indeed, Figure 8f displays that the MnO_2 attach to the surface of RGO, instead of aggregating themselves.

Figure 9 demonstrates the fabrication of the flexible asymmetric SC. Figure 9a and b show SEM images of the cross-section of MnO_2/RGO and RGO films with the graphite current collector on the top surface. They both have a layer-by-layer structure, which benefits from the pilling of 2D MnO_2 and RGO, or just RGO. The cross-section SEM images of the assembled SC (Figure 10c and d) show a sandwich-like structure. To achieve a high flexibility of final device, the thicknesses of both electrodes are limited to a few tens of micrometers as well as the gel electrolyte after the compression (Figure 10d).

BC/PAAS- Na_2SO_4 plays a significant role in flexible SCs, where two electrodes have to be sticked with each other by gel electrolyte, but prevented from the short circuit (Figure 10). The BC clusters soaked by PAA gel (Figure

10e) take the responsibility for the separation. The image of BC/PAAS- Na_2SO_4 and its rheology behavior are demonstrated in Figure 10f. It shows a very high viscosity ($\sim 10^4$ Pa s) and low dependence on the temperature. High viscosity and sticky property of gel electrolyte can combine two electrodes together, preventing from the split-up under the cycling of bending.

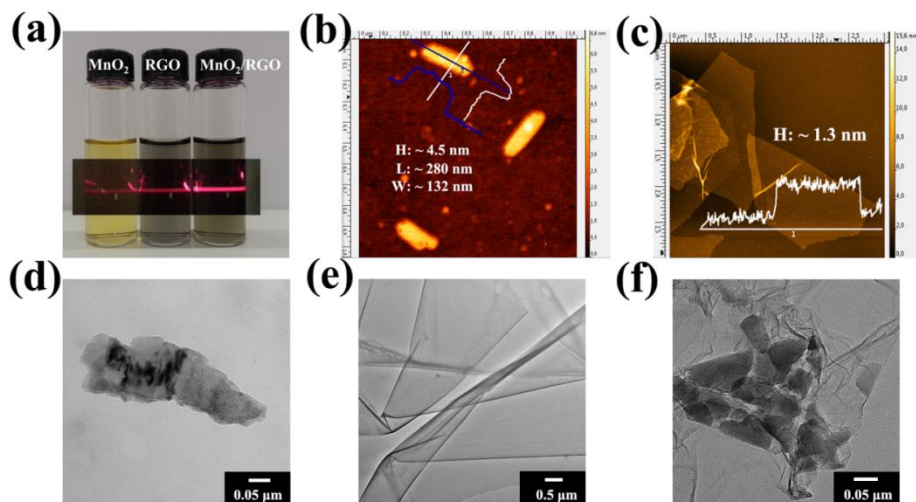


Figure 8 (a) Photograph of the aqueous colloidal suspensions of MnO_2 , RGO and MnO_2/RGO , showing Tyndall effect when the red laser goes through, AFM images of (b) MnO_2 and (c) RGO, TEM images of (e) MnO_2 , (f) RGO and (g) MnO_2/RGO .

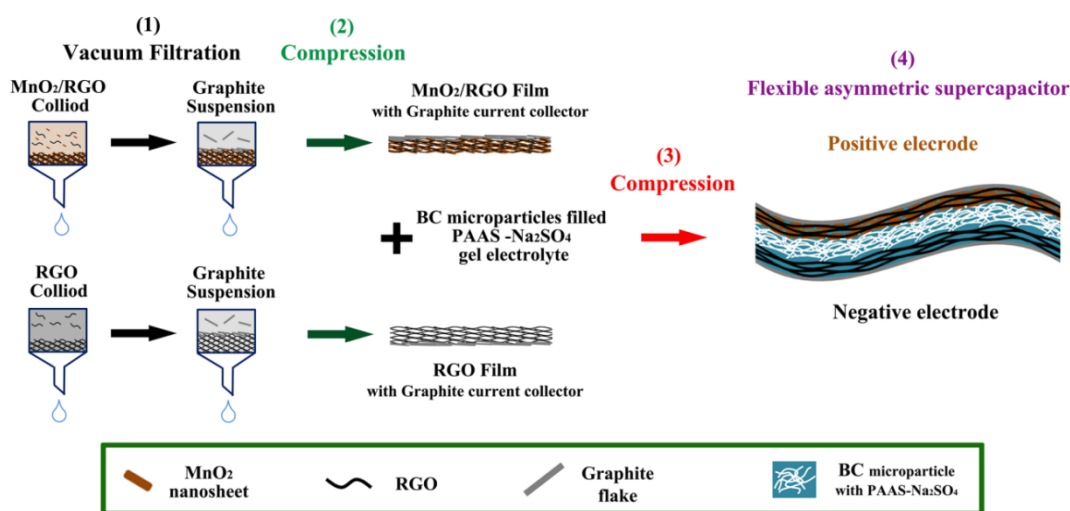


Figure 9 Schematic illustration of the preparation process. (1) Vacuum filtration of MnO_2/RGO , RGO colloidal suspensions and graphite flakes suspension, (2) Compression to obtain MnO_2/RGO and RGO hydrogel films with attached graphite current collector, (3) Compression to assemble the flexible SC with obtained hydrogel films and BC/PAAS- Na_2SO_4 gel electrolyte, (4) Schematic structure of the assembled flexible asymmetric SC, demonstrating the role of separation of BC clusters.

First of all, cyclic voltammetry was used to estimate the potential window of each electrode (MnO_2/RGO and RGO) in a three-electrode system (Figure 11a).

The stable potential window is between -1.0 and 0 V for RGO and between 0 and 0.8 V for MnO₂/RGO, which indicates the fabricated cell can achieve an extended potential range of 1.8 V. To obtain such operating voltage, to keep the amount of charges, Q, stored in the positive and negative electrodes the same is necessary. It can be expressed by the following equation:

$$Q = C_{sp}^+ \times m^+ \times \Delta U^+ = C_{sp}^- \times m^- \times \Delta U^-$$

where ΔU^+ and ΔU^- , represent the potential window of positive and negative electrodes, respectively, during the operation of the SC. Thus the mass ratio of two electrodes can be calculated by the equation:

$$m^-/m^+ = C_{sp}^+ \times \Delta U^+ = C_{sp}^- \times \Delta U^-$$

since the C_{sp}^+ of MnO₂/RGO is 164 F g⁻¹ and the C_{sp}^- of RGO is 87 F g⁻¹ calculated from the CV profiles in Figure 11a, the weight ratio (m^-/m^+) of RGO and MnO₂/RGO was kept to 1.5 in the asymmetric SC cell according to the above equation.

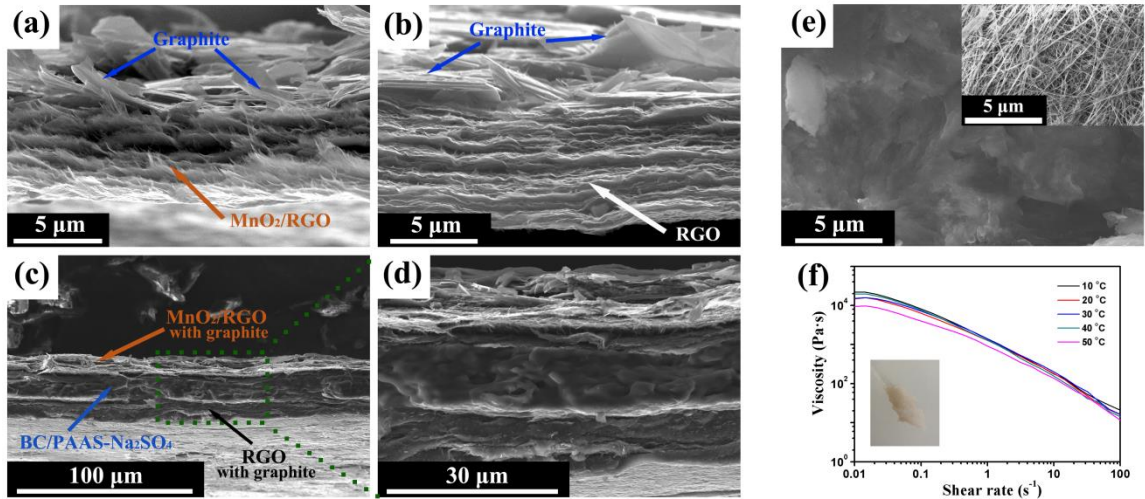


Figure 10 SEM images of the cross-section of MnO₂/RGO (a) and RGO (b) hydrogel films with graphite current collectors, and (c) the assembled SC and (d) at high magnification, and (e) the BC/PAAS-Na₂SO₄ gel electrolyte (inset image shows the BC nanofibers in BC cluster), (f) effect of the viscosity of BC/PAAS-Na₂SO₄ gel electrolyte on shear rate at various temperatures (Inset shows the digital image of this gel electrolyte).

As expected, the fabricated asymmetric SC can achieve a wide voltage up to 1.8 V shown in Figure 11b. Galvanostatic charge/discharge curves at different current densities in a potential window of 0 - 1.8 V (Figure 11c) indicate that this asymmetric SC has an excellent capacitive behavior with rapid I-V response. The specific capacitance (C_t) of the asymmetric SC is calculated to be 27 F g⁻¹ (C_A , 29 mF cm⁻²) based on the total mass of active materials in the two electrodes at a current density of 0.5 A g⁻¹ and still reaches 17 F g⁻¹ (18 mF cm⁻²) at a high current density of 10 A g⁻¹. Ragone plots, depicting the relation

between power density (P) and energy densities (E), were used to evaluate the performance of the three types of SCs, RGO//RGO, MnO₂/RGO//MnO₂/RGO symmetric, and MnO₂/RGO//RGO asymmetric SCs (Figure 11e). The energy density of MnO₂/RGO//RGO asymmetric SCs (1.8 V) is much higher than those of RGO//RGO, MnO₂/RGO//MnO₂/RGO symmetric SCs (1 V and 0.8 V, respectively). In addition, MnO₂/RGO//RGO exhibits excellent cycling stability. This cell shows good capacitance retention of 85.5 % over the highest capacitance after 5000 cycles.

Because of the optimized structural design, mainly the reduction of the thickness of the final device (about 120 μm including the PE substrates) by thinning both of the electrodes and gel electrolyte, this asymmetric SC exhibits a high flexibility and an excellent cycling stability on the deformation. Figure 12a show its CV curves in different deformation states. CV curves exhibit a similar rectangle shape and only a slight shifting can be observed. In addition, the capacitance retentions of the device after bending and rolling for various times are presented in Figure 12c. There is no significant decrease of specific capacitance occurring, which indicates no huge damage has taken place during the cycling test. Figure 12d shows a packing cell with two MnO₂/RGO//RGO asymmetric SCs in series (3.6 V), which is able to light a light-emitting diode (LED) lamp with a forward voltage of 2.7 V. The rolling of the flexible SC has no obvious effect on the performance of the LED.

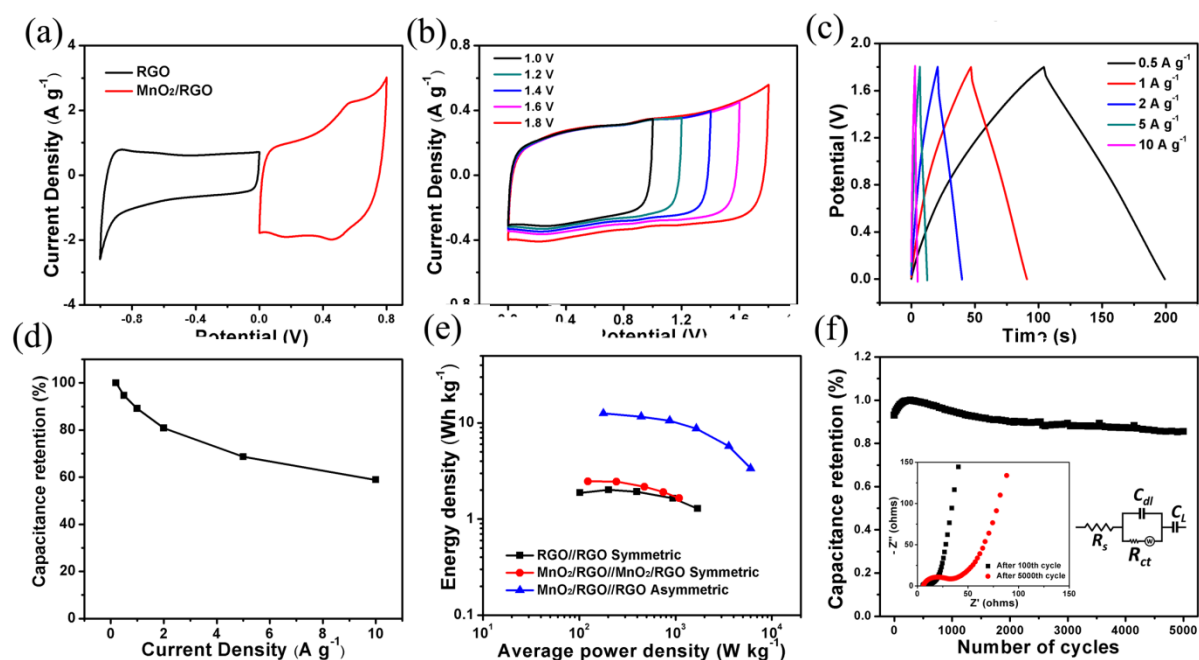


Figure 11 (a) CV curves of RGO and MnO₂/RGO at a scan rate of 10 mV s⁻¹ collected in a three-electrode system with an Ag/AgCl reference in 1 M Na₂SO₄. Electrochemical performance of the assembled flexible asymmetric SC of MnO₂/RGO//RGO: (b) CV curves at a scan rate of 10 mV s⁻¹ with different potential window, (c) Galvanostatic charge-discharge curves at various current densities from 0.5 A g⁻¹ to 10 A g⁻¹, (d) Capacitance retention as a function of discharge currents. (e)

Ragone plots of the asymmetric cell of $\text{MnO}_2/\text{RGO}/\text{RGO}$ (1.8 V), the symmetric ones of RGO/RGO (1 V) and $\text{MnO}_2/\text{RGO}/\text{MnO}_2/\text{RGO}$ (0.8 V). (f) Cycling stability of $\text{MnO}_2/\text{RGO}/\text{RGO}$ at a current density of 1 A g^{-1} (Inset image shows Nyquist plots before and after 5000 cycles, and the electrical equivalent circuit used for fitting impedance spectra).

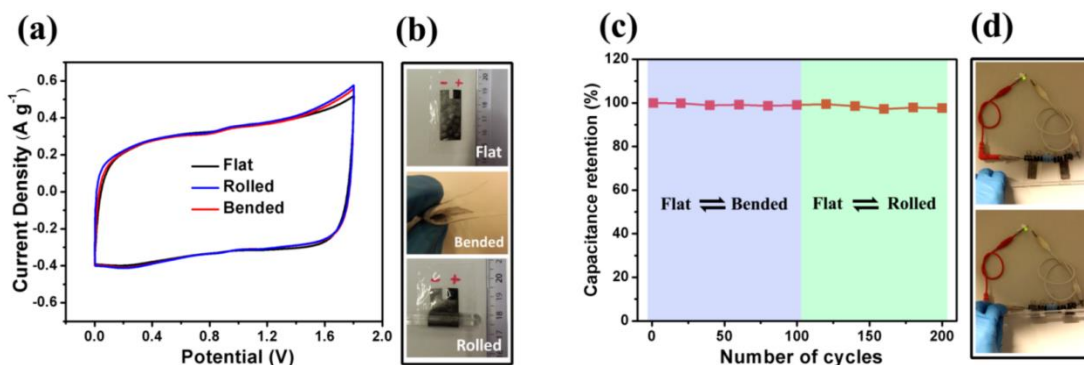


Figure 12 Flexibility of asymmetric $\text{MnO}_2/\text{RGO}/\text{RGO}$ device. (a) CV curves at 10 mV s^{-1} at three different bending state: (b) flat, bended and rolled. (c) Capacitance retention after cycles of repeating flat/bended and flat/rolled. (d) Photograph displays a green light-emitting diode (LED) lighted by two asymmetric cells in series and demonstrates no obvious performance change of LED from the flat state to rolled state.

6.3 In-situ preparation of bacterial cellulose reinforced hydrogel electrolyte for flexible supercapacitors

In this study, one bacterial cellulose (BC) reinforced hydrogel electrolyte with a double network structure created by PAA and SA is reported. The PAA network was covalently crosslinked by poly(ethylene glycol) diacrylate (PEGDA), while the SA network was ionically crosslinked by Ca^{2+} . Moreover, BC clusters, a biopolymer with an inherent network structure, was also added to reinforce further its mechanical property. Finally, a flexible SC was achieved directly by in-situ preparation of this hydrogel electrolyte on two RGO hydrogel based flexible electrodes. The resultant hydrogel electrolyte demonstrates an improved mechanical property and promising performance in flexible SCs.

The schematic diagram in Figure 13 demonstrates the methodology of the preparation of this BC reinforced hydrogel electrolyte. It has a double-network. The first network is created by chemically crosslinked PAA. The crosslink agent is PEGDA (average M_n 250), which has a much longer polymer chain than common crosslinker, N,N' -Methylenebis (acrylamide). It tends to soften the obtained PAA network, which is served as the 'soft' part in this double-network. The second network is constructed by SA, served as the 'hard' part. In order to get a well-connected SA network, two steps of crosslinking were applied. The first step of crosslinking was achieved by CaSO_4 . After the capture of SA gel into the PAA hydrogel, a low but uniform crosslinked SA network generates due to the slow release of Ca^{2+} ions of CaSO_4 . The second step of crosslinking of SA

was completed by massive Ca^{2+} with fast mobility in CaCl_2 solution, which can dramatically increase the degree of crosslinking. The pre-crosslink by CaSO_4 ensures the process of second crosslinking, preventing from the shrinking and nonuniform crosslinking. Moreover, the BC clusters were added to entanglement the chains of these double-network to further enhance the mechanical property.

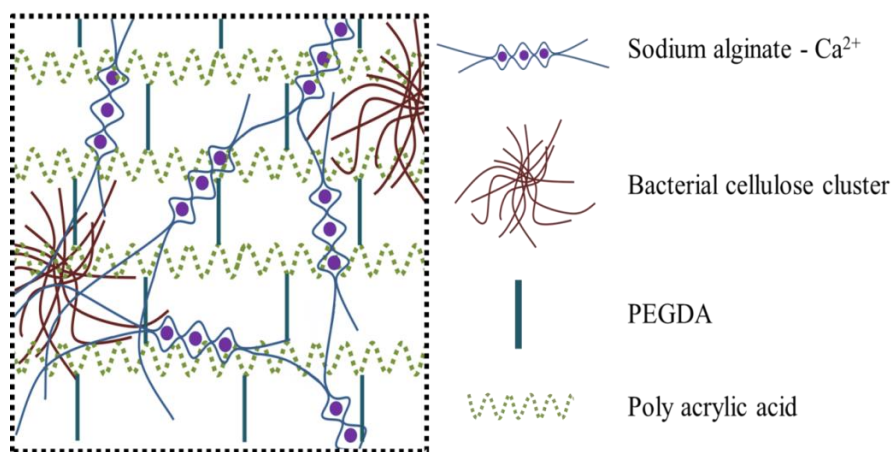


Figure 13 Schematic diagram of the internal structure of PAA/SA-Ca/BC hydrogel, showing the double-network of PAA and Ca^{2+} cross-linked SA and the entanglement by BC clusters.

The morphology of PAA/SA-Ca and PAA/SA-Ca/BC shows that both the hydrogels exhibit high porous structure. In case of PAA/SA-Ca/BC, BC clusters present in the network, acting as knots, which indicates that BC improve the mechanical property. PAA/SA-Ca/BC exhibits more uniform porous structure. A uniform and highly porous structure endows hydrogel electrolytes (PAA/SA-Ca/BC) having a high ionic conductivity as well.

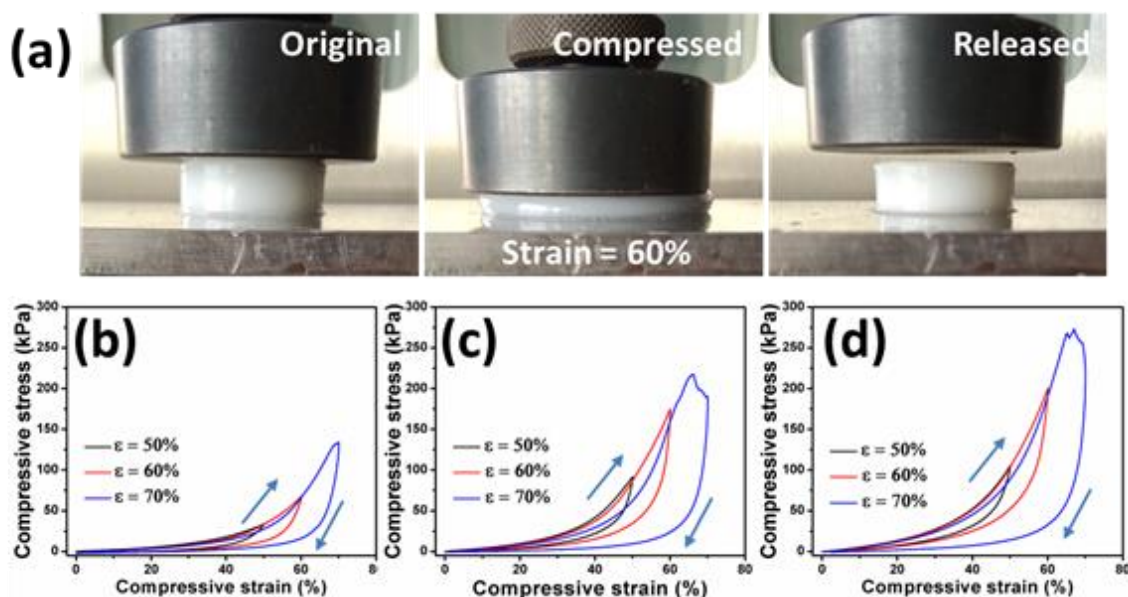


Figure 14 Compressive mechanical properties of prepared hydrogel electrolytes. (a) Images of compressive process of PAA/SA-Ca/BC hydrogel. Compressive stress as a

function of strain from cycling compressive test of (b) PAA/SA-CaSO₄, (c) PAA/SA-Ca and (d) PAA/SA-Ca/BC

Figure 14(a) shows the process of compressive test using an example of PAA/SA-Ca/BC hydrogel. The hydrogel was compressed to the required strain and then released to the initial state. Several cycles (strain = 50 %, 60 % and 70 %) have been conducted until the hydrogel being fractured. PAA/SA-Ca/BC hydrogel exhibits excellent compressive property with a strain of 60 % (Figure 14(a)). Three samples exhibit similar compressive behaviors (Figure 14(b), (c) and (d)). They have good reversibility within strains of 50 % and 60 % and break down when the strain goes up to 70 %. However, the maximum compressive stress of each cycle is different. With the assistance of further ionic crosslink of CaCl₂, PAA/SA-Ca achieved a compressive stress up to 217 kPa compared to PAA/SA-CaSO₄ of 134 kPa. Moreover, with the reinforcement of BC clusters, PAA/SA-Ca/BC exhibits a compressive stress of 273 kPa.

After the in-situ preparation, PAA/SA-Ca/BC hydrogel electrolyte wraps two RGO/G flexible electrodes, combining them together. This SC demonstrates some flexibility. However, due to the high thickness (around a centimeter), the flexibility is limited. What is worse, there is low adhesion between the hydrogel electrolyte and flexible electrodes. During the bending, it tends to be several individual layers. In the further study, the reduction of the thickness of hydrogel electrolyte and the enhancement of the connection of hydrogel through the electrode layer are suggested.

Ionic conductivity of PAA/SA-Ca/BC was measured by electrochemical impedance spectroscopy (EIS) and calculated using the following equation: $\sigma_0 = L/RA$, where L , R and A are the thickness, bulk resistance and area of the hydrogel electrolyte, respectively. The ionic conductivity of PAA/SA-Ca/BC is 0.035 S cm⁻¹ compared to that of 2 M KCl (0.04 S cm⁻¹). The CV curves of assembled SCs with electrolyte of 1 M KCl, 2 M KCl and PAA/SA-Ca/BC, respectively shows that Rare difference is observed between these three electrolytes. Their Nyquist plots indicate that the prepared PAA/SA-Ca/BC hydrogel electrolyte has a very similar electrochemical performance to their liquid electrolytes.

6.4 Summary and outlook

Throughout the text, several conclusions and suggestions are given in this section, helpful to the further study of flexible SCs.

First, porous structure of RGO hydrogel enhances the ions' diffusion without decreasing SSA. It is a simple approach to obtain porous structural RGO without assisted templates. The obtained RGO hydrogel could be an ideal conductive matrix for other pseudo-capacitive materials to deposit on the surface. To this end, the diffusion of monomers has to be considered to make sure a uniform coating of pseudo-capacitive materials from the surface to the internal of RGO

hydrogel. This kind of prepared RGO composite hydrogel seems to be excellent electrode for SCs. However, for its low mechanical property, despite that several strategies were implemented in this study as well as others; more efforts have to be done in the future for its practical application in flexible electrodes.

The importance of current collectors should be highlighted. Direct deposition of ultrathin current collectors on free-standing electrodes is considered to be promising. For RGO hydrogel, because of the water absorbed, it is difficult for them to connect to the circuit. In this study, graphite current collector can directly deposit on its surface by intercalated into the stand-up RGO nanosheets. It is also promising to be the transition layer between RGO and metal current collector for a better contact to enhance the power of prepared SC devices.

Flexible electrodes' thickness can be reduced by using 2D nanomaterials because of the layer-by-layer pilling. In the case of RGO hydrogel, the reduction of the thickness may not be that significant due to the separation of water molecular. And a certain degree of restacking is necessary to improve the mechanical property. Thus, it is suggested to use restacked 2D nanomaterials with high specific capacitance and well controlled deposited thickness. In order to solve the weak ion diffusion, the planar configuration and etching methods for preparing of micro interdigitated electrodes are recommended.

In the sandwich-type configuration, the separation and the combination of two flexible electrodes are both important for the gel/hydrogel electrolyte to achieve. For gel electrolytes, the challenge is the separation, while for hydrogel electrolyte is the combination. For both of them, the reduction of their thickness is essential. In this study, the obtained PAAS- Na_2SO_4 /BC gel electrolyte has played a good role in both aspects. It works well on the function of separation in RGO hydrogel based electrodes, which has a flat surface. It is worthy to study its performance in the flexible electrodes with rough surface.

Finally, by using thinner and softer flexible substrate increases the flexibility of the obtained electrodes. However, the reduction of other properties such as elongation, anti-puncture and abrasion resistance could take a risk in the protection of the electrodes. In addition, the location of the flexible SCs in the integrated circuit board or other device should be considered, because it changes the mechanical neutral plane which is significant to prevent from the fragmentation of electrodes.

BIBLIOGRAPHY

[1] Nathan A., Ahnood A., Cole M. T., Lee S., Suzuki Y., Hiralal P., Bonaccorso F., Hasan T., Garcia-Gancedo L., Dyadyusha A., Haque S., Andrew P., Hofmann S., Moultrie J., Chu D., Flewitt A. J., Ferrari A. C., Kelly M. J., Robertson J., Amaratunga G. A. J. and Milne W. I., *Flexible Electronics: The*

- Next Ubiquitous Platform*. Proceedings of the IEEE, [online]. 2012, vol. 100, issue Special Centennial Issue, pp. 1486-1517. Available from: 10.1109/JPROC.2012.2190168.
- [2] Zhou G., Li F. and Cheng H.-M., *Progress in flexible lithium batteries and future prospects*. Energy Environ. Sci., [online]. 2014, vol. 7, issue 4, pp. 1307-1338. Available from: 10.1039/c3ee43182g.
- [3] Wen L., Li F. and Cheng H.-M., *Carbon Nanotubes and Graphene for Flexible Electrochemical Energy Storage: from Materials to Devices*. Adv. Mater., [online]. 2016, vol. 28, issue 22, pp. 4306-4337. Available from: 10.1002/adma.201504225.
- [4] Xiong C., Li T., Zhao T., Dang A., Li H., Ji X., Jin W., Jiao S., Shang Y. and Zhang Y., *Reduced graphene oxide-carbon nanotube grown on carbon fiber as binder-free electrode for flexible high-performance fiber supercapacitors*. Composites Part B: Engineering, [online]. 2017, vol. 116, issue pp. 7-15. Available from: <http://dx.doi.org/10.1016/j.compositesb.2017.02.028>.
- [5] Wang G., Sun X., Lu F., Sun H., Yu M., Jiang W., Liu C. and Lian J., *Flexible Pillared Graphene-Paper Electrodes for High-Performance Electrochemical Supercapacitors*. Small, [online]. 2012, vol. 8, issue 3, pp. 452-459. Available from: 10.1002/sml.201101719.
- [6] Xu Y., Lin Z., Huang X., Liu Y., Huang Y. and Duan X., *Flexible Solid-State Supercapacitors Based on Three-Dimensional Graphene Hydrogel Films*. ACS Nano, [online]. 2013, vol. 7, issue 5, pp. 4042-4049. Available from: 10.1021/nm4000836.
- [7] Peng X., Peng L., Wu C. and Xie Y., *Two dimensional nanomaterials for flexible supercapacitors*. Chem. Soc. Rev., [online]. 2014, vol. 43, issue 10, pp. 3303-3323. Available from: 10.1039/C3CS60407A.
- [8] Pandolfo T., Ruiz V., Sivakkumar S. and Nerkar J., *General Properties of Electrochemical Capacitors*, Wiley-VCH Verlag GmbH & Co. KGaA, 2013, 9783527646661
- [9] Brousse T., Taberna P.-L., Crosnier O., Dugas R., Guillemet P., Scudeller Y., Zhou Y., Favier F., Bélanger D. and Simon P., *Long-term cycling behavior of asymmetric activated carbon/MnO₂ aqueous electrochemical supercapacitor*. J. Power Sources, [online]. 2007, vol. 173, issue 1, pp. 633-641. Available from: 10.1016/j.jpowsour.2007.04.074.
- [10] Zhang L. L. and Zhao X. S., *Carbon-based materials as supercapacitor electrodes*. Chemical Society Reviews, [online]. 2009, vol. 38, issue 9, pp. 2520-2531. Available from: 10.1039/B813846J.
- [11] Wang G., Zhang L. and Zhang J., *A review of electrode materials for electrochemical supercapacitors*. Chem. Soc. Rev., [online]. 2012, vol. 41, issue 2, pp. 797-828. Available from: 10.1039/c1cs15060j.
- [12] El-Kady M. F., Ihms M., Li M., Hwang J. Y., Mousavi M. F., Chaney L., Lech A. T. and Kaner R. B., *Engineering three-dimensional hybrid supercapacitors and microsupercapacitors for high-performance integrated*

- energy storage*. Proc. Natl. Acad. Sci. U. S. A., [online]. 2015, vol. 112, issue 14, pp. 4233-8. Available from: 10.1073/pnas.1420398112.
- [13] Long J. W., Bélanger D., Brousse T., Sugimoto W., Sassin M. B. and Crosnier O., *Asymmetric electrochemical capacitors—Stretching the limits of aqueous electrolytes*. MRS Bull., [online]. 2011, vol. 36, issue 07, pp. 513-522. Available from: 10.1557/mrs.2011.137.
- [14] Taberna P.-L. and Simon P., *Electrochemical Techniques*, Wiley-VCH Verlag GmbH & Co. KGaA, 2013, 9783527646661
- [15] Gleskova H., Cheng I. C., Wagner S. and Suo Z., *Mechanical Theory of the Film-on-Substrate-Foil Structure: Curvature and Overlay Alignment in Amorphous Silicon Thin-Film Devices Fabricated on Free-Standing Foil Substrates*, Springer Science & Business Media, 2009, 978-0-387-74362-2
- [16] Suo Z., Ma E. Y., Gleskova H. and Wagner S., *Mechanics of rollable and foldable film-on-foil electronics*. Appl. Phys. Lett., [online]. 1999, vol. 74, issue 8, pp. 1177-1179. Available from: 10.1063/1.123478.
- [17] Mao L., Meng Q., Ahmad A. and Wei Z., *Mechanical Analyses and Structural Design Requirements for Flexible Energy Storage Devices*. Advanced Energy Materials, [online]. vol. issue pp. n/a-n/a. Available from: 10.1002/aenm.201700535.
- [18] Zhang H., Qiao Y. and Lu Z., *Fully Printed Ultraflexible Supercapacitor Supported by a Single-Textile Substrate*. ACS Appl. Mater. Interfaces, [online]. 2016, vol. 8, issue 47, pp. 32317-32323. Available from: 10.1021/acsami.6b11172.
- [19] Xu C., Xu B., Gu Y., Xiong Z., Sun J. and Zhao X. S., *Graphene-based electrodes for electrochemical energy storage*. Energy & Environmental Science, [online]. 2013, vol. 6, issue 5, pp. 1388-1414. Available from: 10.1039/C3EE23870A.
- [20] Li D., Muller M. B., Gilje S., Kaner R. B. and Wallace G. G., *Processable aqueous dispersions of graphene nanosheets*. Nat. Nanotechnol., [online]. 2008, vol. 3, issue 2, pp. 101-5. Available from: 10.1038/nnano.2007.451.
- [21] Maiti U. N., Lim J., Lee K. E., Lee W. J. and Kim S. O., *Three-dimensional shape engineered, interfacial gelation of reduced graphene oxide for high rate, large capacity supercapacitors*. Adv Mater, [online]. 2014, vol. 26, issue 4, pp. 615-9, 505. Available from: 10.1002/adma.201303503.
- [22] Feng X., Chen W. and Yan L., *Reduced graphene oxide hydrogel film with a continuous ion transport network for supercapacitors*. Nanoscale, [online]. 2015, vol. 7, issue 8, pp. 3712-3718. Available from: 10.1039/C4NR06897A.
- [23] Moussa M., Zhao Z., El-Kady M. F., Liu H., Michelmoré A., Kawashima N., Majewski P. and Ma J., *Free-standing composite hydrogel films for superior volumetric capacitance*. Journal of Materials Chemistry A, [online]. 2015, vol. 3, issue 30, pp. 15668-15674. Available from: 10.1039/C5TA03113C.
- [24] Tang Q., Sun M., Yu S. and Wang G., *Preparation and supercapacitance performance of manganese oxide nanosheets/graphene/carbon nanotubes*

- ternary composite film*. *Electrochim. Acta*, [online]. 2014, vol. 125, issue pp. 488-496. Available from: 10.1016/j.electacta.2014.01.139.
- [25] Jiang J., Li Y., Liu J., Huang X., Yuan C. and Lou X. W., *Recent advances in metal oxide-based electrode architecture design for electrochemical energy storage*. *Adv Mater*, [online]. 2012, vol. 24, issue 38, pp. 5166-80. Available from: 10.1002/adma.201202146.
- [26] Peng L., Peng X., Liu B., Wu C., Xie Y. and Yu G., *Ultrathin two-dimensional MnO₂/graphene hybrid nanostructures for high-performance, flexible planar supercapacitors*. *Nano Lett.*, [online]. 2013, vol. 13, issue 5, pp. 2151-7. Available from: 10.1021/nl400600x.
- [27] Tao J., Liu N., Ma W., Ding L., Li L., Su J. and Gao Y., *Solid-state high performance flexible supercapacitors based on polypyrrole-MnO₂-carbon fiber hybrid structure*. *Sci Rep*, [online]. 2013, vol. 3, issue pp. 2286. Available from: 10.1038/srep02286.
- [28] Gao H. and Lian K., *Proton-conducting polymer electrolytes and their applications in solid supercapacitors: a review*. *RSC Adv.*, [online]. 2014, vol. 4, issue 62, pp. 33091-33113. Available from: 10.1039/C4RA05151C.
- [29] Anothumakkool B., Torris A. T A., Bhange S. N., Unni S. M., Badiger M. V. and Kurungot S., *Design of a High Performance Thin All-Solid-State Supercapacitor Mimicking the Active Interface of Its Liquid-State Counterpart*. *ACS Applied Materials & Interfaces*, [online]. 2013, vol. 5, issue 24, pp. 13397-13404. Available from: 10.1021/am404320e.
- [30] Yang X., Zhang F., Zhang L., Zhang T., Huang Y. and Chen Y., *A High-Performance Graphene Oxide-Doped Ion Gel as Gel Polymer Electrolyte for All-Solid-State Supercapacitor Applications*. *Advanced Functional Materials*, [online]. 2013, vol. 23, issue 26, pp. 3353-3360. Available from: 10.1002/adfm.201203556.
- [31] Eigler S., Enzelberger-Heim M., Grimm S., Hofmann P., Kroener W., Geworski A., Dotzer C., Rockert M., Xiao J., Papp C., Lytken O., Steinruck H. P., Muller P. and Hirsch A., *Wet chemical synthesis of graphene*. *Adv. Mater.*, [online]. 2013, vol. 25, issue 26, pp. 3583-7. Available from: 10.1002/adma.201300155.
- [32] Kai K., Yoshida Y., Kageyama H., Saito G., Ishigaki T., Furukawa Y. and Kawamata J., *Room-Temperature Synthesis of Manganese Oxide Monosheets*. *J. Am. Chem. Soc.*, [online]. 2008, vol. 130, issue 47, pp. 15938-15943. Available from: 10.1021/ja804503f.
- [33] Cong H.-P., Ren X.-C., Wang P. and Yu S.-H., *Flexible graphene-polyaniline composite paper for high-performance supercapacitor*. *Energy & Environmental Science*, [online]. 2013, vol. 6, issue 4, pp. 1185-1191. Available from: 10.1039/C2EE24203F.

List of figures

<i>Figure 1 Rational design of supercapacitor electrodes with high energy and high power</i>	8
<i>Figure 2 A multilayer film structure bending into a cylindrical roll.</i>	10
<i>Figure 3 Schematic comparison of the sandwich-type supercapacitor (left) and planar supercapacitor (right).</i>	11
<i>Figure 4 SEM images of the surface of RGO hydrogel from (a) top view and (b) side perspective, (c) the surface of graphite side of RGO/G film (inset image shows its high magnification image), (d) the surface of PANI/RGO hydrogel and (e, f) at high magnification, (g) the cross-section of PANI/RGO hydrogel and (h, i) at high magnification.</i>	16
<i>Figure 5 (a) Schematic diagram of PANI/RGO/G hydrogel film on a PET substrate and the different extensions upon the radius caused by bending. (b) Free-movement configuration and its mechanism to reduce the stress force during bending. (c) Illustration for constructing flexible supercapacitor devices using a free-movement configuration (cross section).</i>	16
<i>Figure 6 Electrochemical performance of symmetric flexible devices using various prepared films.</i>	17
<i>Figure 7 Flexibility of PANI/RGO/G device using a free-movement configuration.</i>	18
<i>Figure 8 (a) Photograph of the aqueous colloidal suspensions of MnO₂, RGO and MnO₂/RGO, showing Tyndall effect when the red laser goes through, AFM images of (b) MnO₂ and (c) RGO, TEM images of (e) MnO₂, (f) RGO and (g) MnO₂/RGO.</i>	20
<i>Figure 9 Schematic illustration of the preparation process.</i>	20
<i>Figure 10 SEM images of the cross-section of MnO₂/RGO (a) and RGO (b) hydrogel films with graphite current collectors, and (c) the assembled SC and (d) at high magnification, and (e) the BC/PAAS-Na₂SO₄ gel electrolyte (inset image shows the BC nanofibers in BC cluster), (f) effect of the viscosity of BC/PAAS-Na₂SO₄ gel electrolyte on shear rate at various temperatures (Inset shows the digital image of this gel electrolyte).</i>	21
<i>Figure 11 (a) CV curves of RGO and MnO₂/RGO at a scan rate of 10 mV s⁻¹ collected in a three-electrode system with an Ag/AgCl reference in 1 M Na₂SO₄. Electrochemical performance of the assembled flexible asymmetric SC of MnO₂/RGO//RGO</i>	22
<i>Figure 12 Flexibility of asymmetric MnO₂/RGO//RGO device</i>	23
<i>Figure 13 Schematic diagram of the internal structure of PAA/SA-Ca/BC hydrogel, showing the double-network of PAA and Ca²⁺ cross-linked SA and the entanglement by BC clusters.</i>	24

List of symbols and abbreviations

RGO	Reduced graphene oxide
EDLCs	Electrochemical double-layer capacitors
MnO ₂	Manganese dioxide
PANI	Polyaniline
SSA	Specific surface area
ECs	Electrochemical capacitors
C	Capacitance
Q	Electric charges
V	Potential difference
A	Area
ϵ_0	Permittivity of free space
ϵ_r	Dielectric constant
E	Energy
P	Power
U _{max.}	Maximum operating voltage
E _{max.}	Maximum energy density
w ₊	Weight of the positive electrode
w ₋	Weight of the negative electrode
C _{SP+}	Gravimetric capacitance of the positive electrode
C _{SP-}	Gravimetric capacitance of the negative electrode
ΔU_+	Potential window of the positive electrode
ΔU_-	Potential window of the negative electrode
U	Operation voltage of the optimized capacitor
C' ₊	Capacitance of positive electrode
C' ₋	Capacitance of negative electrode
SWG	Signal waveform generator
CV	Cyclic voltammetry
GCD	Galvanostatic charge/discharge
EIS	Electrochemical impedance spectroscopy
R _s	Solution resistance
ϵ_{top}	Strain in the top surface of the film
d _f	Thickness of the deposited film
d _s	Thickness of the substrate
Y _f	Young's moduli of the deposited film
Y _s	Young's moduli of the substrate
PDMS	Poly(dimethyl siloxane)

GO	Graphene oxide
PVDF	Polyvinylidene fluoride
PVA	Poly(vinyl alcohol)
PET	Polyethylene terephthalate
PE	Polyethylene
KPS	Potassium persulfate
BC	Bacterial cellulose
PEGDA	Poly(ethylene glycol) diacrylate
SA	Sodium alginate
PAAS	Polyacrylic acid sodium salt
C_A	Areal capacitance of each device
A	Footprint area of the electrodes.
C_{sc}	Specific capacitance of one electrode in two electrode system
XPS	X-ray photoelectron spectroscopy
SEM	Scanning electron microscopy
AMF	Atomic force microscopy
XRD	X-ray diffraction
G_{app}	Apparent G peak
2D	Two-dimensional
PAA	Polyacrylic acid
CMC	Sodium carboxymethyl cellulose
PAAM	Polyacrylamide
σ_0	Ionic conductivity
L	Thickness of the hydrogel electrolyte,
R	Block resistance of the hydrogel electrolyte
A	Area of of the hydrogel electrolyte

List of publications

1 Fei, H.; Saha, N.; Kazantseva, N.; Moucka, R.; Cheng, Q.; Saha, P., A Highly Flexible Supercapacitor Based on MnO₂/RGO Nanosheets and Bacterial Cellulose-Filled Gel Electrolyte. *Materials* 2017, 10 (11), 1251.

2 Fei, H.; Saha N.; Kazantseva N.; Babkova T.; Machovsky M.; Wang G.; Bao H.; Saha P. Polyaniline/Reduced Graphene Oxide Hydrogel Film with Attached Graphite Current Collector for Flexible Supercapacitors. *Journal of Materials Science: Materials in Electronics* **2017**, doi: 10.1007/s10854-017-8233-3

Conference proceedings cited in Web of Science/Scopus

1 Fei, H.; Saha, N.; Kazantseva, N.; Wang, G. C.; Bao, H.; Saha, P., A strong and sticky hydrogel electrolyte for flexible supercapacitors. In *Proceedings of the Regional Conference Graz 2015 - Polymer Processing Society PPS:*

Conference Papers, Holzer, C. H.; Payer, M., Eds. Amer Inst Physics: Melville, 2016; Vol. 1779. ISBN: 978-0-7354-1441-9

2 Fei, H.; Saha, N.; Zandraa, O.; Moučka, R.; Kazantseva, N.; Wang, G.; Bao, H.; Saha, P. In situ preparation of bacterial cellulose reinforced hydrogel electrolyte for flexible supercapacitors, NANOCON 2016 - Conference Proceedings, 8th International Conference on Nanomaterials - Research and Application, 2016; pp 583-587. ISBN: 978-80-87294-71-0

3 Shah, R.; Vyroubal, R.; **Fei, H. J.**; Saha, N.; Kitano, T.; Saha, P., Preparation of Bacterial Cellulose Based Hydrogels and Their Viscoelastic Behavior. In Novel Trends in Rheology Vi, Zatloukal, M., Ed. Amer Inst Physics: Melville, 2015; Vol. 1662. ISBN: 978-0-7354-1306-1

Curriculum Vitae

Name:	Haojie FEI
Date of birth:	9 th November 1987
Place of birth:	Pinghu, Zhengjiang, China
Permanent address:	Feizhang 24, Guangcheng, Pinghu
Affiliation:	Centre of Polymer system, Faculty of Technology, Tomas Bata University in Zlin, Nám. T. G. Masaryka 5555, 760 01 Zlín
Telephone:	(+420) 773176408
E-mail:	haojie@utb.cz
Education	<p>2014 – to date Tomas Bata University in Zlin, Faculty of Technology, Ph.D. studies in Chemistry and Materials Technology, Specialization: Technology of Macromolecular Compounds.</p> <p>2010 – 2013 East China University of Science and Technology, Shanghai (China), Master`s degree in Materials Science and Engineering.</p> <p>2006 – 2010 Zhejiang University of Science and Technology, Hangzhou (China), Bachelor`s degree in Materials Science and Engineering.</p>

**Fabrication of flexible supercapacitors with
high electrochemical performance**

Výroba flexibilního superkondenzátoru s vysokým elektrochemickým výkonem

Doctoral Thesis Summary

Published by: Tomas Bata University in Zlín

nám. T. G. Masaryka 5555, 760 01 Zlín

Edition: published electronically

Typesetting by: Haojie FEI

This publication has not undergone any proofreading or editorial review.

Publication year: 2018

First Edition

ISBN 978-80-7454-725-6

